Investigations of the Structure, Topology, and Interactions of the Transmembrane Domain of the Lipid-Sorting Protein p24 Being Highly Selective for Sphingomyelin-C18

Christopher Aisenbrey, Patricia Kemayo-Koumkoua, Evgeniy Salnikov, Elise Glattard, Burkhard Bechinger

Biochemistry

Article

pubs.acs.org/biochemistry

Investigations of the Structure, Topology, and Interactions of the Transmembrane Domain of the Lipid-Sorting Protein p24 Being Highly Selective for Sphingomyelin-C18

Christopher Aisenbrey,[†] Patricia Kemayo-Koumkoua,[†] Evgeniy S. Salnikov, Elise Glattard, and Burkhard Bechinger*

Université de Strasbourg/CNRS, UMR7177, Institut de Chimie, 4, rue Blaise Pascal, 67070 Strasbourg, France

Supporting Information

ABSTRACT: The p24 proteins play an important role in the secretory pathway where they selectively connect various cargo to other proteins, thereby being involved in the controlled assembly and disassembly of the coat protein complexes and lipid sorting. Recently, a highly selective lipid interaction motif has been identified within the p24 transmembrane domain (TMD) that recognizes the combination of the sphingomyelin headgroup and the exact length of the C18 fatty acyl chain (SM-C18). Here, we present investigations of the structure, dynamics, and sphingomyelin interactions of the p24 transmembrane region using circular dichroism, tryptophan fluorescence, and solid-state nuclear magnetic resonance (NMR) spectroscopies of the polypeptides and the surrounding lipids. Membrane insertion and/or conformation of the TMD is strongly dependent on the membrane lipid composition where the transmembrane helical insertion is strongest in the presence of 1-palmitoyl-2-oleoyl-*sn*-glycero-3-phosphocholine (POPC) and SM-C18. By analyzing solid-state NMR angular restraints from a large number of labeled sites, we have found a tilt angle of 19° for the transmembrane helical domain at a peptide-to-lipid ratio of 1 mol %. Only minor changes in the solid-state NMR spectra are observed due to the presence of SM-C18; the only visible alterations are associated with the SM-C18 recognition motif close to the carboxy-terminal part of the hydrophobic transmembrane region in the proximity of the SM headgroup. Finally, the deuterium order parameters of POPC-d_{31} were nearly unaffected by the presence of SM-C18 or the polypeptide alone but decreased noticeably when the sphingomyelin and the polypeptide were added in combination.

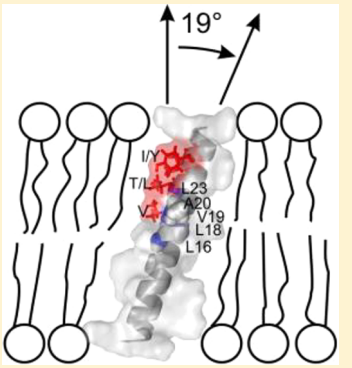

The secretory pathway is essential in the synthesis, transport, and processing of proteins and bioactive molecules and plays a key role in intercellular communication.[1] Thereby, it is vitally important and can be linked to a variety of diseases. A well-functioning secretory pathway assures the controlled transport and sorting of proteins and lipids along subcompartments of the endoplasmic reticulum, the Golgi apparatus, and the plasma membrane. During the early secretory pathway, the combination of anteriograde and retrograde transport by vesicles covered by coat protein I and II (COPI- and COPII-coated transport vesicles, respectively) and sorting ensure a controlled and tunable system assuring the correct amount, processing, and destination of proteins and lipids in each compartment.[1,2]

COPI vesicles ensure the retrograde transport of the early secretory pathway by shuttling from the early Golgi back to the endoplasmic reticulum.[1] Interestingly, these vesicles are depleted of cholesterol and sphingomelin (SM) except for one SM species carrying a C18 fatty acyl chain providing evidence for an early segregation and sorting of these lipids.[3] The vesicles are made of an outer heptameric coatomer showing similarities to the clathrin coat, the p24 family of proteins that connect to various cargos in a selective manner, and a number of proteins that mediate contact between these layers and are involved in the controlled assembly and disassembly of the complexes.[1,2,4,5]

The p24 proteins exist in mammals, yeast, and plants and are involved in cellular signaling, hormone secretion, and the occurrence of Alzheimer's disease.[5] They have also been shown to be important during the development of mice embryos.[6] Lipid cross-linking experiments in cells using a radioactive sphingolipid precursor and immunoprecipitation revealed a strong interaction of the sphingolipid with p24 but not with p23, another member of the family.[7] In follow-up experiments, the transmembrane domains of p23 and p24 were prepared as fusions with maltose binding proteins and reconstituted into model membranes and their interactions with pentaenoyl-shingomyelins were investigated by FRET.[8,9] Distinct FRET was observed for the Trp4 residue of the p24 transmembrane domain with SM-C18:5 but not for p23. Furthermore, the FRET signal was considerably weaker in the presence of sphingomyelins with different chain lengths or for the corresponding phosphatidylcholine (PC-C18:5) indicating a highly specific

Received: April 26, 2019
Revised: May 22, 2019
Published: May 23, 2019

DOI: 10.1021/acs.biochem.9b00375
Biochemistry XXXX, XXX, XXX−XXX

interaction of the p24TMD and SM-C18. An alanine scanning experiment revealed a number of residues that represent a structural motif for lipid selectivity. These are all positioned at the carboxy-terminal end of the TMD and on the same face of the helix. MD simulations indeed show transient interactions of SM-C18 with p24 involving these amino acid residues with a lifetime of the complex in the range of 250 ns.[8]

Whereas the modulation of protein activity by sphingolipids and their binding to proteins has previously been characterized,[10] the selection of a molecular species based on headgroup and fatty acyl chain composition is rather unique.[8] It has been shown that sphingomyelin-C18 modulates the inactive monomer to active oligomer equilibrium of p24,[8] thereby regulating its interactions with cargo and/or other proteins of the COPI complex.[2] An allosteric mechanism of regulation has been suggested in which polar residues involved in dimer formation are localized opposite the SM-C18 molecular recognition motif.[10] A bioinformatics analysis identified related shingomyelin recognition motifs of the type [V/I/T/L]XX[V/I/T/L][V/I/T/L]XX[V/I/T/L][F/W/Y] in a wide variety of membrane proteins, including the major histocompatibility complex II Qα-chain or GPCRs, in particular within helix 6.[11] The bulky β-branched residues and the aromatic residues of the motif form a crevice recognized by SM-C18.

To gain better insight into the lipid interactions of p24 here, we used circular dichroism, fluorescence, and oriented solid-state NMR spectroscopies to investigate the structure, topology, and dynamics of the p24 transmembrane domain in phospholipid bilayers. We also tested for conformational and/or topological changes that may occur due to interactions with SM-C18.

Solid-state NMR spectroscopy of uniaxially oriented lipid bilayers is a well-established technique for the investigation of the topology of membrane-associated polypeptides.[12−15] When several orientation-dependent parameters have been measured, accurate helix topologies have been determined.[12,14,16−18] In particular, the combination of oriented solid-state NMR spectra of ^{15}N-labeled peptide bonds with methyl-deuterated alanines provides a sensitive measure of the topology of the membrane-associated helices where changes in the tilt and rotational pitch angles of as little as 1° become apparent.[19−21] Furthermore, the line shapes of the backbone and side chains are indicators of motional averaging and structural heterogeneity.[22−24]

The peptides were reconstituted in various phospholipid model membranes, including complex mixtures that represent well the lipid composition of the Golgi membranes.[8] Finally, the changes in the lipid alignment and fatty acyl chain order parameters due to the presence of p24TMD and/or the SM have been monitored using ^{31}P and ^{2}H solid-state NMR spectroscopy;[25−27] thus, a complete picture of the p24−lipid supramolecular arrangement is obtained.

By combining several biophysical approaches and a good number of isotopic labeling schemes, the work presented here reveals important structural details such as the secondary structure, helix tilt angle, side chain dynamics, and protein−lipid interactions, and only minor changes in the p24TMD structure and dynamics were observed upon addition of SM-C18 to supported phosphatidylcholine bilayers.

■ MATERIALS AND METHODS

Organic solvents were purchased from Sigma-Aldrich (St. Louis, MO) with a purity of 99%; cholesterol and phospholipids, including *N*-octadecanoyl-D-erythro-sphingosylphosphorylcholine (SM-C18), were purchased from Avanti Polar Lipids (Birmingham, AL). Fmoc amino acids were from NovaBiochem/Merck KGaA (Darmstadt, Germany), and isotope-labeled amino acids from Cortecnet (Voisins les Bretonneux, France) or Aldrich (St. Louis, MO). TentaGel-R-RAM resin was from Rapp Polymer GmbH (Tübingen, Germany).

Peptide Synthesis. The human p24TMD peptides with the sequence KKTNS RVVLW SFFEA LVLVA MTLGQ IYYLK R-CONH$_2$ (UniProt entry Q15363 TMED2_HUMAN, residues 165−193 and two additional lysines at the amino terminus) were prepared by solid phase peptide synthesis using an automatic Millipore 9050 synthesizer, TentaGel-R-RAM resins (Rapp Polymer GmbH), and a 4-fold excess of Fmoc-protected amino acid (NovaBiochem/Merck KGaA). Isotope-labeled peptides were prepared using ^{15}N- and ^{2}H-labeled amino acids (Cortecnet) incorporated at chosen positions. After cleavage and deprotection in a trifluoroacetic acid (TFA)/water/triethylsilane mixture [28/1.5/0.3 (v/v/v)], the peptide in solution was taken up in toluene [50/50 (v/v)] and the solvent evaporated. The peptide was washed three times in cold ether at 4 °C. The peptide was purified by semipreparative reverse phase HPLC using Prontosil 300-6-C4 5.0 μm (Bischoff, Leonberg, Germany) or Luna 100-C18 5.0 μm columns (Phenomenex) and an acetonitrile/water gradient. The purity of p24TMD was tested by analytical HPLC, and the identity was verified by matrix-assisted laser desorption ionization mass (MALDI) spectrometry. The final yields of the pure peptide were typically 10% with a loss of ∼83% during the purification step. The dry peptide pellet was solubilized in 4% acetic acid to exchange the counterions and lyophilized.

The peptides with the following isotopic labels were synthesized: ^{15}N-Leu23 and $^{2}H_8$-Val19, ^{15}N-Val19 and $^{2}H_{10}$-Leu23, ^{15}N-Leu23 and $^{2}H_3$-Ala20, ^{15}N-Ala20, ^{15}N-Leu18 and $^{2}H_3$-Ala20, ^{15}N-Val19 and $^{2}H_3$-Ala15, ^{15}N-Leu18 and $^{2}H_3$-Ala15, and ^{15}N-Leu16 and $^{2}H_3$-Ala15. Notably, here the numbering of residues includes the full peptide and thereby adds +6 when compared to the numbering of ref 8. The corresponding positions of the full-length protein are obtained by adding +162 to the numbering used here.

Reconstitution in Liposomes. On the basis of extensive reconstitution assays,[28,29] proteoliposomes were prepared in the following manner. Aliquots of 30 μM peptide in water were prepared from a 1 mg/mL stock solution, and the water was removed by lyophilization; 100 μL of a 10 mM stock solution of lipid in hexafluoroisopropanol (HFIP) was added to the lyophilized peptide, and the mixture completed with solvent to give a final volume of 1 mL. After vortexing, the solvents were evaporated under a stream of nitrogen gas. The remaining traces of solvent were removed by high vacuum overnight. The resulting film was hydrated in 10 mM phosphate buffer (pH 7). Small unilamellar vesicles (SUVs) were obtained by tip sonication at 4 °C (Sonoplus HD 200; Bandelin, Berlin, Germany). Aggregates and titanium debris from the tip were removed at room temperature by centrifugation for 30 min at 11000*g*.

Reconstitution in Detergent. A stock solution of peptide was prepared in water; samples were diluted to a final concentration of 30 μM, and the water was removed by lyophilization overnight. The peptide was dissolved again in HFIP, and the solvent was evaporated under a stream of nitrogen gas and under vacuum overnight. Thereafter, it was resuspended in 10 mM phosphate buffer (pH 7). Detergent stock solutions of *n*-dodecylphosphocholine (DPC) and SDS

DOI: 10.1021/acs.biochem.9b00375
Biochemistry XXXX, XXX, XXX−XXX

were prepared at final concentrations of 10 and 100 mM, respectively, and diluted to different concentrations ranging from 0.1 to 16 mM during peptide titrations.

Circular Dichroism. CD spectra were recorded from 30 μM peptide solutions (and 1 mM lipid were applicable) in 300 μL cuvettes (Hellma Analytics, Mühlheim, Germany) on a Jasco (Tokyo, Japan) J-510 spectropolarimeter using a scan speed of 50 nm/min, a bandwidth of 3 nm, and five scans collected covering the range from 250 to 190 nm using a quartz cell with a 1 mm path length, at 25 °C. The spectra were processed using the spectra manager software of the instrument, and the solvent contributions subtracted. Secondary structures were analyzed with the CDpro Web server using the CONTINLL algorithm.[30]

Tryptophan Fluorescence. The intrinsic fluorescence of p24TMD due to the presence of a tryptophan was measured using a FluoroLog spectrophotometer (HORIBA, Ltd., Kyoto, Japan) with the polarization filters always at the magic angle. Fluorescence emission spectra were recorded from 295 to 455 nm at an excitation wavelength of 280 nm. The excitation slit width was 1 nm; the emission slit width was 4 nm. The peptide was prepared in 10 mM phosphate buffer (pH 7.2) at a final concentration of 30 μM. A series of emission spectra were recorded at 25 °C while samples were being stirred.

Preparation of Oriented Samples for Solid-State NMR Spectroscopy. Selectively labeled ^{15}N and/or ^{2}H p24TMD was first dissolved in HFIP, and the solvent was removed under a stream of nitrogen. The peptide was then dissolved in a 50/50 (v/v) HFIP/water mixture and added in a stepwise manner to ∼150 mg of POPC in HFIP with a final peptide-to-lipid (P/L) molar ratio of 1%. Thereafter, the solvent was gently evaporated under a stream of nitrogen to decrease its total volume to ∼0.5 mL. To avoid peptide aggregation, small volumes of HFIP were added; thus, the water content remained low during the process.[28] The resulting clear and viscous sample that was deposited onto ∼20 ultrathin glass plates (6 mm × 11 mm or 8 mm × 22 mm, thickness 00, i.e., ∼80 μm, Paul Marienfeld, Lauda-Königshofen, Germany) slowly dried in air, and the residual solvent evaporated under high vacuum. After the sample had equilibrated at 93% humidity for 2−3 days at room temperature, the glass plates were stacked on top of each other. The stack was stabilized by Teflon tape, and the sample sealed in plastic wrapping to avoid dehydration.

Preparation of Non-Oriented Samples. Non-oriented samples were prepared by dissolving 3 mg of deuterated POPC (POPC-d_{31}) and 0.14 mg of p24TMD (1 mol %; pH adjusted to 7) and/or 0.15 mg of SM-C18 (5 mol %) in HFIP. The solvent was evaporated under a stream of nitrogen and high vacuum overnight; thus, a film forms on the walls of the small glass tube (6 mm outer diameter). The sample was then resuspended in 15 μL of 10 mM phosphate buffer (pH 7.1) by vortexing and sonication in a water bath followed by five freeze/thaw cycles. In some cases, stable vesicles were obtained only after a drying and resuspension step. For NMR spectral acquisition, the glass tube with the sample was directly inserted into the solenoidal coil of a static solid-state NMR probe.

Solid-State NMR Experiments. Solid-state NMR spectra were recorded on a Bruker Avance NMR spectrometer operating at 9.4 T (some spectra were acquired at 7.05 T). The oriented samples were inserted into commercial E-free flat coil NMR probes (Bruker, Rheinstetten, Germany) with the normal parallel to the magnetic field.[31] All spectra were recorded at 295 K.

Proton-decoupled ^{15}N solid-state NMR spectra were recorded at 40.54 MHz on a Bruker Avance NMR 400 MHz spectrometer using a cross-polarization (CP) pulse sequence. The CP contact time was 800 μs, the repetition time 3 s, the ^{1}H B_1 field 31 kHz, and the spectral width 38 kHz, and the acquisition times ranged from 6 to 20 ms. The spectra were calibrated relative to external ammonium chloride ($^{15}NH_4Cl$) at 40 ppm.[32] An exponential apodization function with a line broadening of 200 Hz was applied prior to Fourier transformation.

Proton-decoupled ^{31}P solid-state NMR spectra were recorded at 161.937 MHz on a Bruker Avance 400 MHz NMR spectrometer using a Hahn-echo pulse sequence,[33] an echo time of 40 μs, a repetition time of 3 s, a ^{31}P B_1 field of 60−80 kHz, and a spectral width of 40−120 kHz. The spectra were referenced relative to 85% phosphoric acid (H_3PO_4) at 0 ppm. An exponential line broadening (LB) of 150 Hz was applied prior to Fourier transformation.

Deuterium solid-state NMR spectra of the $^{2}H_3$-alanine-labeled peptide reconstituted in lipid bilayers were recorded at 61.4 MHz on a Bruker Avance 400 MHz NMR spectrometer using a quadrupole-echo sequence.[34] A dwell time of 1 μs was chosen to allow a precise adjustment of the echo by left-shifting the FID after the acquisition (corresponding to a spectral window of 500 kHz); a B_1 field of 30−50 kHz, an acquisition time of 8 ms, interpulse delays of 30−50 μs, and a recycling time of 1.5 s were used. For processing, the FID was left-shifted to the top of the echo. An exponential multiplication corresponding to a LB of 500 Hz was applied before Fourier transformation. All ^{2}H solid-state NMR spectra were referenced relative to external $^{2}H_2O$ at 0 ppm.

For ^{2}H solid-state NMR spectra of deuterated lipids, a repetition delay of 0.3 s, an echo time of 100 μs, a dwell time of 0.5 μs, and a B_1 field of 40 kHz were used. The processing included an exponential apodization with a line broadening of 100 Hz. The temperature was set to 37 °C.

Calculation of Angular Restraints from Experimental Solid-State NMR Spectra. To determine the peptide orientations that agree with the experimental spectra, a coordinate system was defined. Within the α-helix, the tilt is defined as the angle between the long axis of the helix and the membrane normal, and the pitch angle as that between the membrane normal and the line within an arbitrary plane of the peptide helical wheel projection. Protein Data Bank (PDB) coordinates of an ideal α-helix were generated in MOLMOL.[35] The coordinates of the labeled ^{15}N atom, the corresponding amide proton, and the C atom of the previous residue were extracted and used to calculate the ^{15}N chemical shift tensor in the same reference frame using the main ^{15}N chemical shift tensors reported previously (55.8, 81.4, and 228.6 ppm).[36] By successively rotating the peptide molecule around the pitch and the tilt angle, we systematically screened the three-dimensional orientational space in 50 × 50 steps using a program written in MATHEMATICA 3.0 (Wolfram Research, Champaign, IL).[19,37] Contour plots mark the angular pairs that agree with the experimental results. The simulation of the ^{2}H solid-state NMR spectra was performed on the same principles by extracting the coordinates of the C_α and C_β atoms in the oriented PDB files. The contour plots of several ^{15}N- and ^{2}H-labeled sites were superimposed in a single plot.

Calculation of the Lipid Order Parameters. To investigate the lipid fatty acyl chain packing and dynamics in the presence of p24, the TMD was reconstituted into liposomes

DOI: 10.1021/acs.biochem.9b00375
Biochemistry XXXX, XXX, XXX−XXX

where the palmitoyl chain of POPC lipids is deuterated throughout. Therefore, the deuterium solid-state NMR spectra from such samples represent several overlapping quadrupolar splittings, each providing information about the order parameter of the deuterated CD_2 and CD_3 sites (see Figure 8). The deuterium order parameters (S_{CD}) of each CD_2 and CD_3 group are extracted according to the equation $S^i_{CD} = \frac{4}{3}\frac{h}{e^2qQ}\Delta^i\upsilon$, where e^2qQ/h is the static quadrupole coupling constant (167 kHz) for a C−D bond.[38]

RESULTS

Preparation of the Synthetic Peptides. To perform structural investigations of the p24 transmembrane domain, a peptide encompassing the hydrophobic membrane anchor and the SM-C18 recognition motif was prepared by solid phase peptide synthesis. Eight additional amino acids of the native human p24 sequence were included as well as two lysines at the amino terminus added to make the peptide more water-soluble (see the sequence shown in Table 1). The yield after purification by semipreparative HPLC using an acetonitrile/water gradient was ~10%, where most of the decrease in yield was associated with the purification step. The purity of the final product was estimated to be ≥90% as determined by analytical HPLC, and its composition was verified by MALDI mass spectrometry (Figures S1 and S2).

Table 1. ^{15}N Chemical Shift Measurements of the p24TMD Reconstituted into Oriented Phospholipid Bilayers of either POPC or the 95/5 POPC/SM Mixture at a Lipid-to-Peptide Ratio of 100[a]

KKTNS RVVLW SFFE**A** **L**V**L**V**A** MT**L**GQ IYYLK R-$CONH_2$

^{15}N label position	^{15}N chemical shift in POPC (ppm)	^{15}N chemical shift in 95/5 POPC/SM (ppm)
L23	218 ± 4	221 ± 3
A20	224 ± 4	224 ± 4
V19	217 ± 4	218 ± 7
L18	206 ± 9	205 ± 8
L16	216 ± 5	216 ± 4
^{2}H$_3$ label position	^{2}H$_3$ quadrupolar splitting in POPC (kHz)	^{2}H$_3$ quadrupolar splitting in 95/5 POPC/SM (kHz)
A15	20 ± 3	20 ± 3

[a]The sequence is indicated with the recognition motif in red, the labeled sites in bold, and the TMD underlined. The indicated range of chemical shifts and quadrupolar splittings represents the line width at 80% maximal intensity and was used for the restriction analysis. The chemical shift maxima can be defined with higher precision (cf. Figure 4A).

p24TMD Secondary Structure in Micelles and Lipid Bilayers. To monitor the secondary structure of the p24TMD in membrane environments, CD spectra of 30 μM p24TMD were recorded upon addition of *n*-dodecylphosphocholine (DPC) or sodium dodecyl sulfate (SDS). Whereas in the absence of a detergent the dichroic spectra were featureless as is often observed for aggregated peptides, minima at 209 and 222 nm quickly appeared upon addition of a detergent (Figure 1A,C). In the case of DPC, a sudden transition occurs between 1.2 and 2 mM, i.e., once the CMC of this detergent is reached (Figure 1A,G).[39] Upon addition of SDS, the helical features appear more slowly in agreement with the higher CMC of this detergent (Figure 1C,G). The corresponding fluorescence spectra indicate that the environment of the p24 tryptophan becomes less polar upon addition of detergents. When DPC is added, the intensity changes are pronounced (2.5-fold) until the CMC is reached while the fluorescence maximum remains at 331 nm (Figure 1B,G). The changes upon titration with SDS are more complex. Whereas the intensity at 331 nm increases by only ~30%, additional spectral intensities appear between 300 and 325 nm (Figure 1D,G). Whereas the use of these detergents offers a first view of the protein structure in membranelike environments, many details about the conformation and lipid interactions require investigations in liquid crystalline phospholipid bilayers.[40]

Therefore, in a next step, the peptides were reconstituted into bilayers of different lipid compositions using a previously developed reconstitution protocol.[28] Liquid crystalline bilayers made of zwitterionic phosphatidylcholines provide simple model systems for eukaryotic membranes where this lipid headgroup is abundant. The hydrophobic thickness of the DMPC, POPC, and POPE membranes corresponds to that of natural eukaryotic membranes; the latter represents well the mixture of saturated and unsaturated fatty acyl chain, by being made from a single component correlating biophysical analysis to the specific characteristics of phospholipids. For example, whereas the cylindrical shape of POPC results in stable bilayer arrangements, the small headgroup of POPE results in negative curvature strain.[41,42]

The CD and fluorescence spectra of p24TMD in POPC or DMPC (Figure 1E,F) are indicative of a helical peptide in a hydrophobic environment similar to the spectra obtained at intermediate DPC concentrations (Figure 1A,B). A $\Theta_{222}/\Theta_{209}$ ratio of >1 is suggestive of significant oligomerization of the peptide in membranes,[43] where the Trp of p24TMD in the saturated DMPC exhibits a somewhat more polar environment.

When 5 mol % SM is included in the POPC bilayers, the helical features and the hydrophobic environment of p24TMD are much increased (Figure 1E,F) and the spectra resemble those of the highest DPC concentrations investigated (Figure 1A,B). In contrast, when samples are reconstituted into POPE membranes, the CD spectra are featureless and the fluorescence spectra are indicative of a rather polar environment with a low quantum yield and an intensity maximum at 302 nm (Figure 1E,F). Interestingly, when a POPC membrane encompassing 10 mol % POPE and 5 mol % SM is investigated, the PE offsets the effects of the SM. As a consequence, the CD and fluorescence spectra are intermediate with respect to those obtained in the presence of DMPC or POPC (Figure 1E,F).

When ^{15}N-labeled peptides are reconstituted in uniaxially oriented samples and investigated with the membrane normal parallel to the magnetic field of the NMR spectrometer, the ^{15}N chemical shifts provide a direct indicator of the approximate tilt angle.[44] Whereas transmembrane helical domains exhibit ^{15}N chemical shifts around 200 ppm, helices that align parallel to the bilayer surface are characterized by chemical shifts of <100 ppm. An accurate determination of the tilt and rotational pitch angles of a polypeptide domain is obtained by combining information from the ^{2}H quadrupolar splitting of $^2H_3$-labeled alanines and the ^{15}N chemical shift of labeled peptide bonds using doubly labeled peptides prepared by chemical peptide synthesis.[20,21,37,45]

Because POPC showed the best results when membrane insertion and structural formation of the p24TMD were tested under a variety of conditions[28,29] and in optical analysis (Figure 1E,F), this lipid was used as a reference to extensively investigate

DOI: 10.1021/acs.biochem.9b00375
Biochemistry XXXX, XXX, XXX−XXX

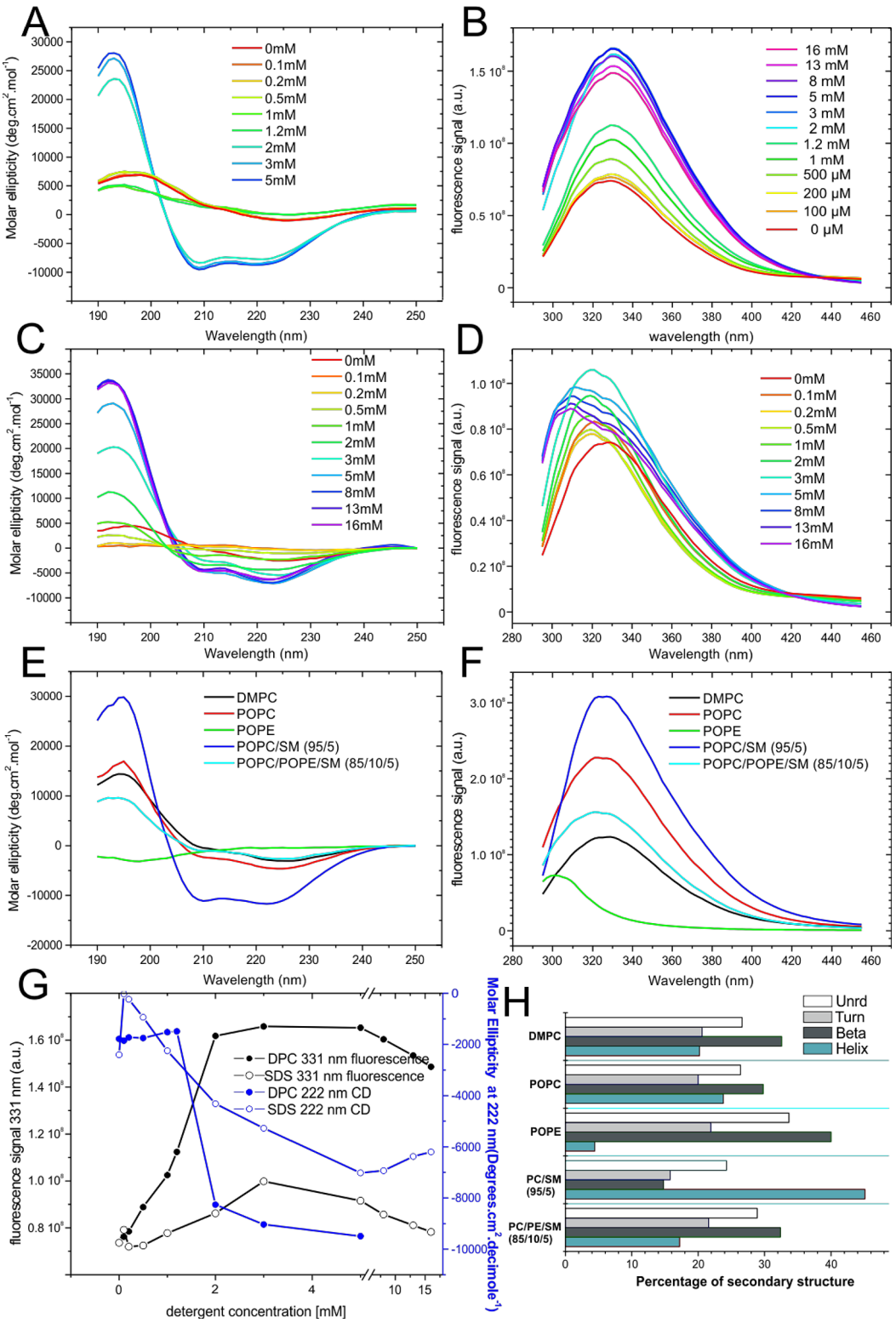

Figure 1. CD and fluorescence spectra of p24TMD in membrane environments. (A, C, and E) CD and (B, D, and F) tryptophan fluorescence spectra of 30 μM p24TMD in 10 mM phosphate buffer (pH 7) in the presence of increasing concentrations of DPC (A and B) or SDS (C and D) or in the presence of small unilamellar vesicles made from the phospholipids indicated at a peptide-to-lipid ratio of 3 mol % (E and F). (G) The fluorescence intensity at 331 nm (black traces) and the molar ellipticity at 222 nm (blue traces) are shown as a function of DPC (filled circles) and SDS (open circles) concentrations (data from panels A–D). (H) Analysis of the secondary structure composition from the spectra shown in panel E using CDPro.[30] The data were recorded at 25 °C except for the spectra in the presence of DMPC (37 °C).

the domain by solid-state NMR spectroscopy. As discussed above, POPC forms stable lipid bilayers and provides a suitable model system for eukaryotic membranes. Several p24TMD peptides were prepared carrying ^{15}N- and $^{2}H_3$-alanine isotopic labels at specific sites (Table 1), reconstituted into oriented POPC membranes at a peptide-to-lipid ratio of 1/100, and f2

DOI: 10.1021/acs.biochem.9b00375
Biochemistry XXXX, XXX, XXX−XXX

investigated by ^{15}N solid-state NMR spectroscopy (Figure 2A–E). Here, we focused on the carboxy-terminal end of the TMD

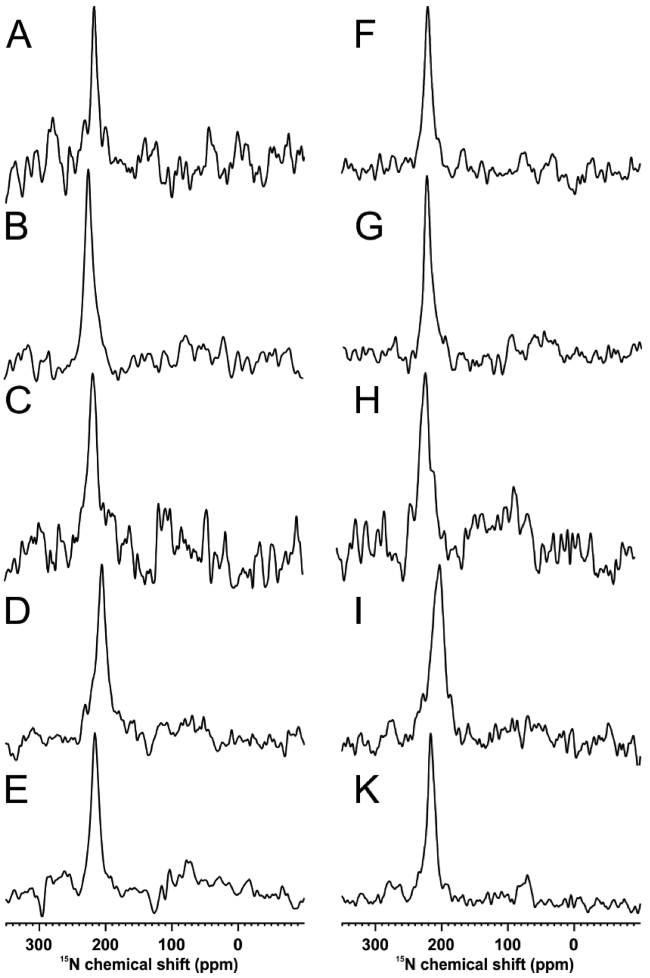

Figure 2. Proton-decoupled ^{15}N solid-state NMR spectra of p24TMD reconstituted into (A–E) oriented POPC or (F–I and K) 95/5 POPC/SM-C18 bilayers at peptide-to-lipid ratios of 1 mol %. The sample was uniaxially aligned with the normal parallel to B_o. The labeled positions are (A and F) ^{15}N-L23 and $^{2}H_3$-A20, (B and G) ^{15}N-A20, (C and H) ^{15}N-V19 and $^{2}H_{10}$-L13, (D and I) ^{15}N-L18 and $^{2}H_3$-A15, and (E and K) ^{15}N-L16 and $^{2}H_3$-A20. The measurements were performed at ambient temperature.

because Val19, Thr22, Leu23, I26, and Tyr27 have been found to be important for the interaction of the TMD with the SM-C18 lipid.[8] The ^{15}N chemical shifts of a number of labeled residues, including sites that are part of the recognition motif or close by, have been determined in successive experiments and are listed in Table 1. The spectra exhibit well-oriented line shapes with chemical shifts between 205 ± 2 and 224 ± 4 ppm, a range that is associated with transmembrane helical alignments (Figure 2A–E). The corresponding ^{31}P NMR spectra show major intensities around 30 ppm indicative of liquid crystalline PC aligned with the normal parallel to the magnetic field. Additional intensities extending to −15 ppm are from lipids that exhibit different headgroup conformations and/or are oriented at other angles, including contributions from the non-oriented sample (representative spectra are shown in Figure 3D–F).[25] In view of the good alignment of the polypeptides as judged from the ^{15}N solid-state NMR spectra, the ^{31}P intensity distribution probably

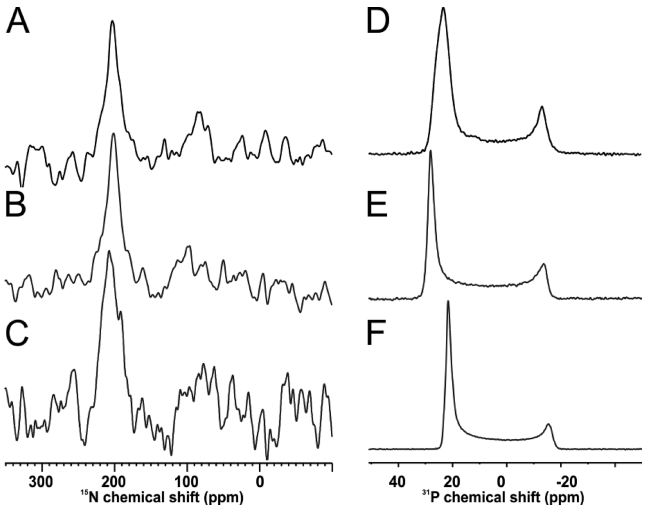

Figure 3. Proton-decoupled ^{15}N solid-state NMR spectra of [^{15}N-L18,$^{2}H_3$-A20]p24TMD reconstituted into (A) oriented POPC, (B) 95/5 POPC/SM-C18, or (C) 90/10 POPC/SM-C18 bilayers at a peptide-to-lipid ratio of 1 mol %. The samples were uniaxially oriented with the normal parallel to B_o. The corresponding ^{31}P solid-state NMR spectra of the same samples are shown in panels D–F, respectively. The measurements were performed at ambient temperature.

reflects an inherent property arising from the TMD–lipid interactions (Figures 2 and 3).

To test for the effect of the sphingolipid, 5 mol % SM was added to the phosphatidylcholine membranes. Closely related ^{15}N spectral line shapes and chemical shifts were observed (Figure 2F–I,K and Table 1). Only the L23 position exhibits a visible chemical shift difference. To further investigate the effect of SM-C18, its content was increased to 10 mol % and the ^{15}N-Leu18 TMD investigated. Indeed, a small increase in the chemical shift maximum by ∼5 ppm and a line broadening effect were observed for the 10% SM sample (Figure 3A–C). The broader line shape indicates a more heterogeneous population of the p24 peptide in these membranes. Interestingly, despite the weak tendency of the ^{15}N label to shift to higher values and/or to cause somewhat broader lines, the ^{31}P chemical shift anisotropies of the SM18-containing samples remain constant or even tend to decrease (Figure 3D–F).

The peptide carrying a ^{15}N-labeled L23 was also reconstituted into an oriented lipid bilayer of a composition that more closely mimics that of the membrane of the Golgi apparatus. The spectrum closely matches that obtained in the presence of a 95/5 POPC/SM mixture (Figure 4A). To compare more closely the effects of SM-C18, Figure 4 shows expansions of the ^{15}N solid-state NMR spectra obtained for the L23, A20, and L16 sites in the presence of POPC or a 95/5 POPC/SM mixture. Whereas the spectra of A20 and L16 superimpose in the absence or presence of SM-C18 (Figure 4B,C), the L23 site shows a small difference in the chemical shift maximum when 5 or 8 mol % SM is present (Figure 4A).

^{2}H Quadrupolar Splittings of Alanines. Whereas the ^{15}N solid-state spectra shown in Figures 2–4 provide a direct indicator of the transmembrane orientation of the p24TMD helix, more accurate topologies are obtained when samples are analyzed in combination with ^{2}H solid-state NMR spectra of alanines that carry deuterons at their methyl group and are located within the same domain.[19] The resulting quadrupolar splitting reports on the alignment of the C_α–C_β bond relative to

DOI: 10.1021/acs.biochem.9b00375
Biochemistry XXXX, XXX, XXX–XXX

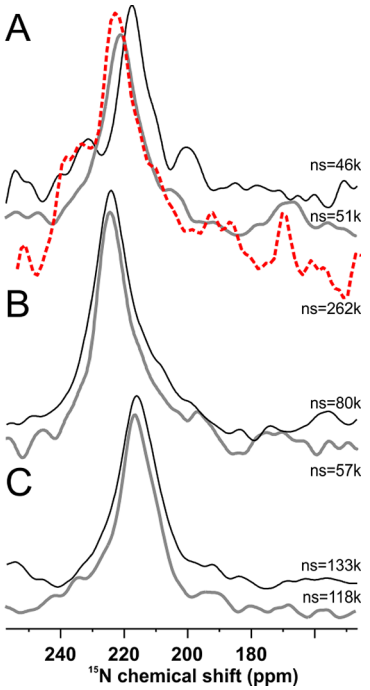

Figure 4. Proton-decoupled ^{15}N solid-state NMR spectra of p24TMD reconstituted into oriented POPC (black lines), 95/5 POPC/SM-C18 (gray lines), or 52/19/5/16/8 POPC/POPE/POPS/cholesterol/SM-C18 bilayers (red hatched line) at a peptide-to-lipid ratio of 1 mol %. The samples were uniaxially aligned with the normal parallel to B_o. The labeled positions are (A) ^{15}N-L23 and $^{2}H_3$-A20, (B) ^{15}N-A20, and (C) ^{15}N-L16 and $^{2}H_3$-A15. The measurements were performed at ambient temperature. The number of scans is indicated for each experiment.

the magnetic field direction as well as the mosaic spread of this angle.[19] When the p24TMD labeled with $^{2}H_3$ at the alanine 15 position was reconstituted into POPC or 95/5 POPC/SM oriented membranes, the ^{2}H solid-state spectra exhibit within experimental error closely related quadrupolar splittings of ~20 ± 1.5 kHz (Figure 5A,B). These values represent a C_α−C_β bond alignment relative to the magnetic field direction (membrane normal) of ~44° or ~67° (depending on whether the splitting has a positive or negative sign). Spectral line shape analysis indicates that the mosaicity of the samples is 7−8° (Figure 5A,B, red lines). When the 95/5 POPC/SM sample is measured at 4 °C, much of the intensity is lost, suggesting exchange processes that occur at intermediate time scales close to the gel-to-liquid crystalline phase transition of the membrane (not shown). The phase transition temperature of pure SM-C18 is 45 °C,[46] and that of POPC −2 °C,[47] where mixtures of phospholipids often show a broad transition in the intermediate range.[48,49]

When the sample is investigated at −20 °C, a spectrum representing a large range of C_α−C_β alignments is obtained (Figure 5C). A predominant transmembrane alignment with little additional intensity between 40 and 100 ppm is observed in the corresponding ^{15}N solid-state NMR spectrum of ^{15}N-Ala15 in POPC.[29] Thus, the peptide remains globally aligned also when the bilayers are frozen (see, e.g., ref 50). The data suggest that the alanine 15 side chain scans a considerable orientational space. Whereas this dispersion is averaged at ambient temperature, it becomes evident at −20 °C.

The ^{2}H solid-state spectra of $^{2}H_3$-alanine 20 after reconstitution into oriented membranes made from POPC, 95/5 POPC/SM, and 90/10 POPC/SM bilayers are shown in panels D−F of Figure 5, respectively. The alanine side chain exhibits an intensity distribution of quadrupolar splittings; however, the overall intensity is relatively low. Therefore, it is difficult to analyze these spectra in further detail, and the simulations in Figure 5D−F are shown to illustrate how even small changes in angles affect the spectral line shapes. In the presence of 5 mol % SM, a single quadrupolar splitting of ~20 kHz (Figure 5E) appears to be suggestive of a more homogeneous alignment under these conditions, although overall the intensity distribution is quite similar to the spectra in the absence or presence of 10% SM-C18 (Figure 5D,F).

Restriction Analysis. The orientational restraints were used to calculate the topology of an ideal helix encompassing the residues listed in Table 1. Whereas one NMR parameter can be used to provide semiquantitative information about the alignment of the domain, they all have to agree with a single tilt and pitch angular pair of a polypeptide domain. To analyze the data in a quantitative manner, all possible alignments of the p24 helix are tested by rotating the TMD in a stepwise manner around the helix axis as well as a perpendicular director. For each alignment thus obtained, the ^{15}N chemical shifts and the ^{2}H quadrupolar splitting are calculated and compared with the experimental values, including their dispersion that has been extracted from the line width at 80% maximal intensity (Table 1). When agreement is obtained with a measurement, the angular pair is labeled on the restriction plot shown in Figure 6A, where the black trace represents the ^{2}H quadrupolar splitting of Ala15 and the colored traces represent the ^{15}N chemical shifts of Leu16 (blue), Leu18 (red), Val19 (green), Ala20 (pink), and Leu23 (turquoise) when reconstituted into uniaxially oriented 95/5 POPC/SM membranes (Table 1). The circle highlights the tilt and pitch angular pair where most measurements coincide. Only the ^{15}N chemical shift of alanine 20 misses this intersection by a few degrees. The corresponding tilt and pitch angles of 19° and 235°, respectively, are represented by the helical structure shown in Figure 6B. Figure 6A also reveals the highly complementary nature of ^{15}N and ^{2}H solid-state NMR measurements.[19]

To further explore the structure and dynamics of the p24TMD side chains, a peptide deuterated at the Leu23 side chain was prepared and investigated. The Leu23 residue is part of the SM-C18 recognition motif[8] (Table 1). The labeled leucine side chain encompasses 10 deuterons, two CD_3 groups, two CD groups at the α- and γ-positions, and a CD_2 at the β-position. Whereas the three deuterons of the methyl group of alanine result in a single quadrupolar splitting that reflects the alignment of the C_α−C_β bond and thus the backbone topology, the situation for most of the leucine deuterons, in particular the six deuterons of the CD_3 groups, is different because of the additional degrees of freedom that arise from combined rotations around the C_α−C_β and C_β−C_γ bonds.[51,52] Therefore, at room temperature, relatively narrow spectral lines are obtained (Figure 7A,B). Slowing these motions at low temperatures results in a much broader intensity distribution ranging over 37 kHz with a different line shape (Figure 7C,D). Under those conditions, the presence of 5 mol % SM results in an ~10% increase in the maximal quadrupolar splitting.

Investigation of p24TMD in a Golgi-like Membrane. As the sorting of SM-C18 in the COPI vesicles involves p24TMD when localized in the Golgi cellular compartment,[3] the polypeptide was also investigated in POPC/POPE/POPS/cholesterol/SM bilayers at a 52/19/5/16/8 molar ratio, thereby more closely mimicking the lipid composition of the Golgi

DOI: 10.1021/acs.biochem.9b00375
Biochemistry XXXX, XXX, XXX−XXX

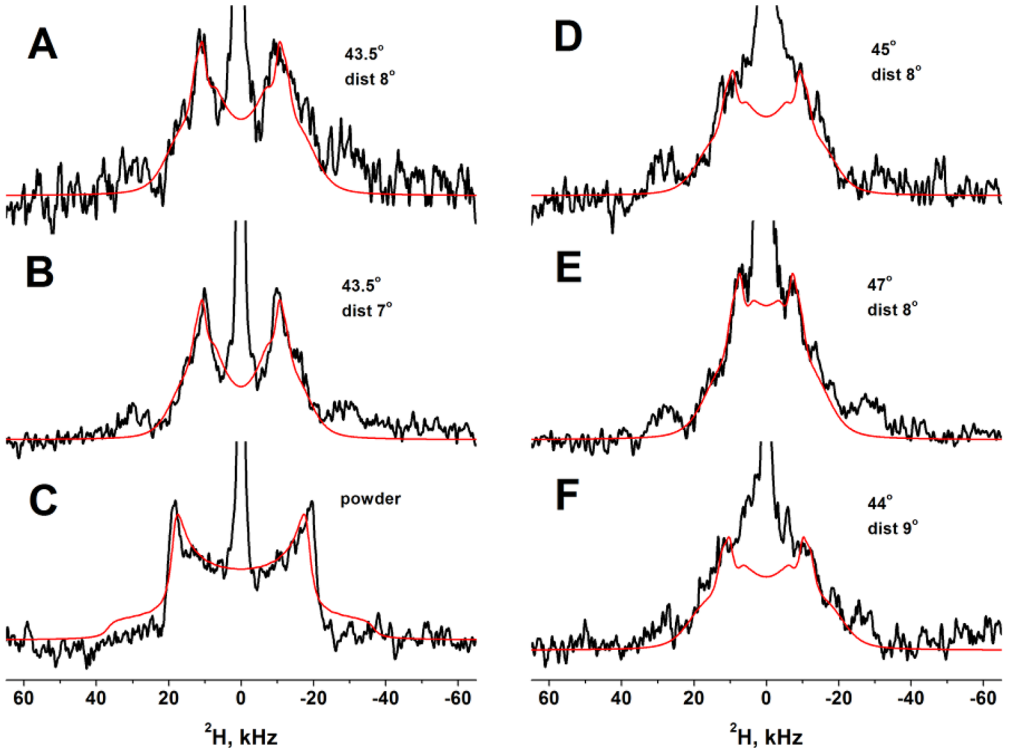

Figure 5. ^{2}H solid-state NMR spectra of p24TMD labeled with $^2H_3$-alanine at the (A−C) A15 or (D−F) A20 site and reconstituted into (A and D) oriented POPC, (B, C, and E) 95/5 POPC/SM-C18, or (F) 90/10 POPC/SM-C18 bilayers at peptide-to-lipid ratios of 1 mol %. The sample was uniaxially oriented with the normal parallel to B_o. The measurements were performed at ambient temperature (A, B, and D−F) or at −20 °C (C). The central peaks are from residual HDO. The interpulse delay in the solid-echo sequence was 50 μs (A−C). The spectra were acquired with 11K (C and D) to 27K (F) scans. The red lines in panels A, B, and D−F show simulated spectra assuming an average alignment relative to the membrane normal (B_o field) with a Gaussian distribution of the C_α−C_β bond. The corresponding angles (in the range of 43.5−47°) and distribution (SDs around 8°) are shown to the right of the spectra. Panel C compares the experimental spectrum to a powder pattern line shape.

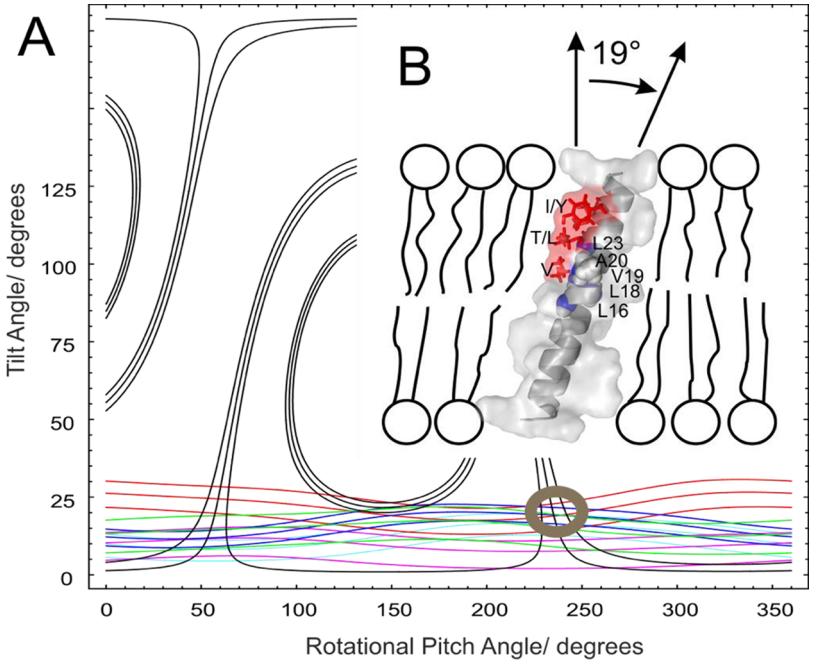

Figure 6. (A) Restriction analysis for the p24TMD topology based on the solid-state NMR measurements shown in panels F−I and K of Figure 2 and Table 1. The orientational restraints from the $^2H_3$-Ala20-labeled site (black) as well as from the ^{15}N measurements of Leu16 (blue), Leu18 (red), Val19 (green) Ala20 (pink), and Leu23 (turquoise) are shown. The circle highlights the topologies around the tilt and pitch angular pair (19° and 235°, respectively) common to all but one orientational restraint. (B) Structural model of p24TMD in a lipid bilayer representing the topology from the restriction analysis of solid-state NMR measurements.

DOI: 10.1021/acs.biochem.9b00375
Biochemistry XXXX, XXX, XXX−XXX

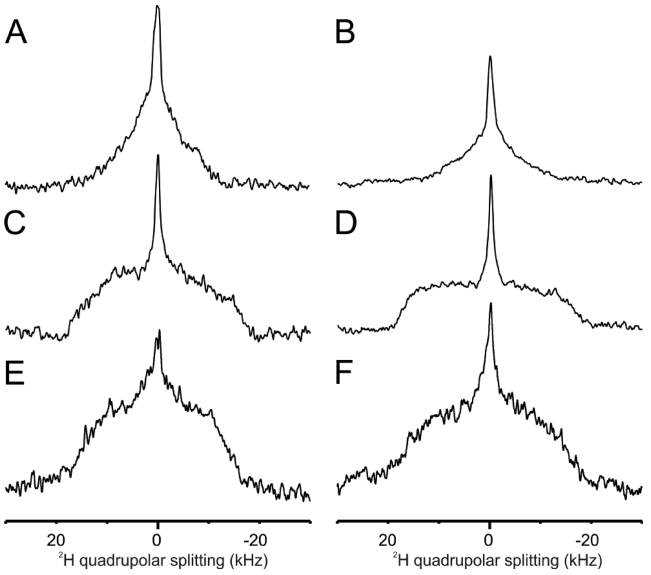

Figure 7. ^{2}H solid-state NMR spectra of p24TMD labeled with (A−D) $^2H_{10}$-leucine at position L23 or (E and F) $^2H_8$-valine at position V19 reconstituted into oriented POPC (A and C), 95/5 POPC/SM-C18 (B and D), 60/19/5/16 POPC/POPE/POPS/Chol (E), and 52/19/5/16/8 POPC/POPE/POPS/Chol/SM-C18 (F) at peptide-to-lipid molar ratios of 1 mol %. The sample was uniaxially oriented with the normal parallel to B_o. The measurements were performed at ambient temperature (A and B), −20 °C (C and D), or 40 °C (E and F). The interpulse delay in the solid-echo sequence was 30 μs.

membrane.[8,53] The ^{15}N solid-state NMR spectra of the peptide labeled at position 23 exhibit a transmembrane chemical shift of 223 ppm (Figure 4A). However, considerable intensities corresponding to different peptide alignments, conformations, or the non-oriented sample were also observed, and the intensity of the signal of the TM peak correspondingly decreased (not shown). The ^{2}H solid-state NMR spectrum of the deuterated valine-d_8 side chain of p24TMD position 19 reconstituted into this more complex membrane is shown in Figure 7F. The spectra are dominated by six deuterons associated with two methyl groups next to two CD groups at the α- and β-positions. The broad spectral line ranging over ∼30 kHz even at higher temperatures is thus indicative of a relatively restricted environment of the valine 19 side chains in the hydrophobic environment and does not change much by freezing the sample to −20 °C[29] (not shown). When 8 mol % SM-C18 of this complex mixture is replaced with POPC, the width of the intensity distribution decreases by ∼10% at 40 °C (Figure 7E) but remains largely unaffected at lower temperatures[29] (not shown).

Investigation of the POPC-d_{31} Order Parameters in the Presence of SM and p24TMD. To investigate the lipid fatty acyl chain packing and dynamics in the presence of SM-C18 and/or p24TMD, liposomes were prepared with POPC lipids deuterated throughout their palmitoyl chain. The deuterium solid-state NMR spectra from such samples encompass several overlapping characteristic quadrupolar splittings, each providing information about the order parameter of the deuterated CD_2 and CD_3 sites (Figure 8A). The deuterium order parameters (S_{CD}) of each C−D bond are extracted directly from these spectra in a position-dependent manner (Figure 8B).

The ^{2}H solid-state NMR spectra of POPC-d_{31} and 95/5 POPC-d_{31}/SM lipid vesicles in the absence of peptides are shown in Figure 8A. The largest quadrupolar splitting that is assigned to the relatively rigid CD_2 groups closest to the glycerol backbone decreases from 25.2 to 24.9 kHz in the presence of 5 mol % SM, while the smallest quadrupolar splitting assigned to the methyl group at the end of the acyl chains within the bilayer core stays unchanged at 2.3 kHz. Thereby, the palmitoyl S_{CD} relative profiles exhibit an only minor effect due to the presence of 5 mol % SM-C18.

When 1 mol % p24TMD was added to POPC-d_{31} membranes, only small disturbances of the ^{2}H quadrupolar splittings comparable with the effect of SM-C18 at 5 mol % are observed (Figure 8A). The largest and smallest quadrupolar splitting are 24.8 and 2.4 kHz, respectively, which correspond to relative order parameters of 0.98 and 1.03, respectively, when considering the ratio with the corresponding order parameters of pure POPC-d_{31} (Figure 8B). In contrast, the addition of p24TMD to 95/5 POPC-d_{31}/SM membranes at 1 mol % has a pronounced influence on the ^{2}H quadrupolar splittings. The outermost quadrupolar splitting decreases to 24.6 kHz, and that of the methyl to 2.16 kHz (Figure 8A). The order parameter profile decreases by ∼7% when the palmitoyl CD_2 segments more deeply buried inside the bilayer are considered (Figure 8B).

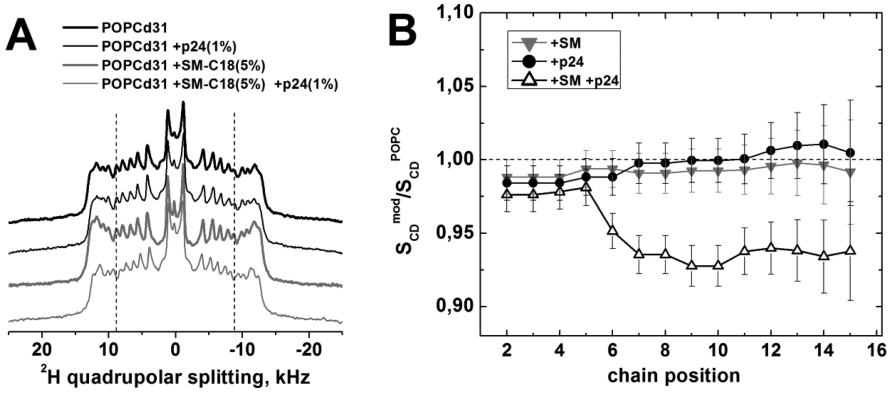

Figure 8. (A) ^{2}H solid-state NMR spectra of POPC-d_{31} (black lines) or 95/5 POPC-d_{31}/SM-C18 vesicles (gray lines) in the absence (thick lines) or presence of 1 mol % p24TMD (thin lines) recorded at 37 °C. (B) The position-dependent relative order parameters of the pure lipids are shown for POPC in the presence of 1 mol % p24TMD (●) and 95/5 POPC/SM bilayers in the absence (▼) or presence of 1 mol % p24TMD (△). The error bars in panel B are propagated by reading out the quadrupolar splitting uncertainties of ±150 Hz.

DOI: 10.1021/acs.biochem.9b00375
Biochemistry XXXX, XXX, XXX−XXX

DISCUSSION

The members of the p24 family of proteins play important roles in the early secretory pathway, i.e., the controlled transport and processing of proteins and lipids within and between the endoplasmic reticulum and the Golgi apparatus.[5] They have been proposed to function as cargo receptors, to provide additional control mechanisms for transport within these intracellular compartments,[1,2] and to be important regulators of transport.[5] Within the p24 transmembrane domain, an amino acid motif that is responsible for very specific interactions with SM carrying a C18 fatty acyl chain has been identified.[8] To the best of our knowledge, this is the only example in which a highly selective protein−lipid interaction has been characterized involving both the headgroup and the fatty acyl chain of lipids. The amino acid motif that assures such preferential interactions with SM-C18 over sphingomyelins carrying shorter or longer fatty acyl chains has been identified to be VXXTLXXIY[8,9] (cf. Table 1). Here we present the first biophysical and structural investigations of p24TMD in phospholipid bilayers and of its lipid interactions.

CD and fluorescence spectroscopic investigations show that after reconstitution into phospholipid bilayers[28] p24TMD adopts a largely helical conformation and its Trp4 is localized in a hydrophobic environment (Figure 1). Whereas the spectroscopic changes correlate with the CMC of detergent micelles (Figure 1A−D,G), the behavior of p24TMD in lipid bilayers is considerably more complex (Figure 1E,F). The helical contributions and the fluorescence intensities are quite pronounced upon reconstitution in POPC bilayers, and this lipid has served as a reference for further comparison. In the presence of DMPC, the helical content was slightly different, although the fluorescence intensity of tryptophan, being at the fourth position of the transmembrane domain, is much decreased. Possibly, due to the location of this residue close to the amino-terminal end of the hydrophobic TMD, the somewhat thinner DMPC membranes expose more of this amino acid to the aqueous environment. A much more pronounced difference is observed when the bilayers were made of POPE carrying a smaller headgroup. Both CD and fluorescence spectroscopy show a different mode of interaction, the peptide possibly tending to oligomerize into larger structures in this environment. Interestingly, the addition of 5 mol % SM considerably increases both the CD helical content of the p24TMD and its fluorescence intensity. The presence of 10% POPE and the presence of 5% SM-C18 largely compensate for each other; thus, the optical parameters are again close to those of pure PC membranes (Figure 1E,F). Thus, the dependence of CD and fluorescence spectra on the lipid headgroup, the membrane thickness, and/or the presence of SM possibly reflects the structural properties of the SM-C18 recognition motif of p24TMD.[8,10] It is noteworthy that the SM headgroup resembles that of PC whereas both SM-C18 and the oleoyl fatty acyl chains of POPC extend over 18 C atoms. Via comparison of the different lipids, both the headgroup and the fatty acyl chain turn out to be important for the p24 transmembrane insertion (Figure 1E,F).

As a next step, the helix topology was determined using solid-state NMR of p24TMD reconstituted into membranes oriented with their long axes parallel to the magnetic field direction of the NMR spectrometer. Whereas under these conditions a set of ^{15}N chemical shifts around 210 ppm (Figures 2−4) are an indicator of transmembrane helix alignments,[44] the highly complementary information obtained from methyl-deuterated alanines (Figure 5) provides detailed information about the helical tilt and pitch angles.[12,21] Thus, a tilt angle of 19° was determined for p24TMD (Figure 6). The same analysis provides a pitch angle of 235°, but the numerical value is dependent on how the corresponding coordinate system was initially defined within the p24 helix. Therefore, Figure 6B also shows the positioning of the labeled amino acids relative to the membrane normal. It should be noted that the ^{15}N chemical shift of alanine 20 misses the common intersection point by a few degrees. However, here an ideal helical conformation encompassing residues 16−23 was assumed. In previous investigations, small adjustments in the helical conformation[54] and/or the introduction of wobbling and rocking motions have been taken into account to reach coincidence.[20] Indeed, the ^{2}H solid-state NMR spectra recorded from the methyl groups of alanine 20 and alanine 15 (Figure 5) indicate an angular distribution of these $C_\alpha-C_\beta$ bonds and thus in the topology and conformation of the sites. With regard to the accuracy of the tilt and pitch angles determined in this manner, we refer to previous investigations in which these angles shifted by a few degrees when motions were taken into consideration or slightly different helical conformations.[20,54] This previous work also presents a detailed analysis of how experimental and systematic errors influence the tilt and pitch angle analysis.

Notably, when the spectra in the absence and presence of SM-C18 are compared to each other (Table 1 and Figures 2−5), there is only little variation in the ^{15}N chemical shifts or $^{2}H_3$-alanine deuterium quadrupolar splittings, indicating that the backbone topology and conformation of p24TMD seem hardly affected by the presence of the sphingomyelin (Figures 2−5 and Table 1). Of the six labeled amino acid residues, two are part of the SM-C18 recognition motif (V19 and L23) whereas others are close by or on the backside of the helix (A15, L16, L18, and A20). The latter have been suggested to be involved in the dimerization of the TMDs.[10] In the presence of 5 or 8 mol % SM-C18, the L23 amide shows some small ^{15}N chemical shift changes (Figure 4A), which represent differences in the angle between the corresponding amide ^{15}NH vector and the B_0 field/membrane normal of ∼2°.[44] Notably, L23 is at the very C-terminal end of the hydrophobic domain, whereas all other residues are more deeply inserted in the low-dielectric part of the lipid bilayer, which is expected to enhance the stability of the H-bonding network.[55] Furthermore, small changes in the dynamics of the Leu23 and Val19 side chains are observed, which were somewhat more restricted in the presence of SM.

The leucine 23-d_{10} spectra are dominated by the six deuterons associated with the two methyl groups not only because of their large number but also because the interpulse delays reduce the signal intensities of the less mobile deuterons of the C_α and C_β positions. Indeed, similar ^{2}H NMR line shapes have been observed when the TM segment of phospholamban was investigated.[51] In this prior work, methyl group rotation about the $C_\gamma-C_\delta$ bond and at 0 °C additional librational motions about the $C_\alpha-C_\beta$ and $C_\beta-C_\gamma$ bonds were used to simulate such line shapes. At −25 °C, the quadrupolar splittings of the three leucines in phospholambdan were 30−36 kHz, while at room temperature, additional 2-fold jumps between predomiant leucine rotamers, fast side chain reorientation, or off axis motions result in further averaging.[51] Although the spectra observed for p24TMD were obtained from macroscopically oriented samples, the degrees of freedom around the $C_\alpha-C_\beta$ and $C_\beta-C_\gamma$ bonds result in an angular distribution of methyl groups approaching that of a powder. Similar to the observations with

DOI: 10.1021/acs.biochem.9b00375
Biochemistry XXXX, XXX, XXX−XXX

the phospholambdan leucines, the ^{2}H NMR spectra of p24TMD leucine 23-d_{10} are suggestive of methyl group rotation and some librational motions, which are more restricted in the presence of SM-C18.

Also, in the case of deuterated valine, comparison with earlier work is of interest. Rotation around the $C_\beta-C_\gamma$ bond results in quadrupolar splittings of ∼35 kHz for both valine-d_6 model compounds or of purple membranes containg γ-d_6-valines over a similar range of temperatures.[56,57] The broad spectral line shapes in these early publications were simulated by fast rotational averaging about the $C_\beta-C_\gamma$ bond. Additional fast averaging about the $C_\alpha-C_\beta$ bond results in quadrupolar splittings of 14 kHz. The width of the ^{2}H spectra suggests that similar motional regimes are present in p24TMD where the presence of SM-C18 has an only minor effect on the spectral line shapes (Figure 7E,F).

Considering that SM-C18−p24TMD interactions have been shown to be highly specific, are associated with a shift in monomer−dimer equilibria of p24 proteins, and are important on a functional level,[5,8,10] one may have expected a more pronounced change in the structural features of p24TMD upon addition of SM-C18. Previously, it was shown that 1 mol % brominated SM-C18 quenches the tryptophan fluorescence of p24-TMD and 0.2 mol % nonbrominated quencher is sufficient to re-establish 50% of the fluorescence (Figure 9 of ref 8), suggesting that there is an excess of SM-C18 in the 5% samples. Of all backbone and side chain spectra investigated here, only the most carboxy-terminal residue L23 exhibited some noticeable changes in both its ^{15}N and ^{2}H solid-state NMR spectra. First, of the labeled sites, only V19 and L23 are part of the motif that has been identified experimentally and simulated to be in contact with the sphingolipid.[8] Whereas L23 may undergo conformational changes due to the proximity of the SM headgroup, V19 is positioned deeper in the membrane where the fatty acyl chains of PC and SM dominate the environment. Second, previous studies have measured a p24 concentration within the cell membranes in the range of 2 ng/nmol lipid concomitant with changes in the monomer−dimer equilibrium when different organelles are compared to each other.[58] This corresponds to a polypeptide-to-lipid ratio of ∼1/10000, which is 100-fold lower when compared to the experimental conditions of our NMR samples. It is thus likely that the p24TMD in the NMR samples is already in its dimeric state even in the absence of SM-C18. Thus, whereas in the cell SM-C18−p24 interactions result in changes in conformation and oligomerization concomitant with an allosteric regulation of activity,[10] the comparatively high P/L ratio in our experiments could promote the dimeric state even in the absence of SM-C18. Indeed, when investigated by SDS−PAGE, the peptides showed a tendency to form oligomers in the absence and presence of POPC or 95/5 POPC/SM bilayers at peptide-to-lipid ratios of 1/100 (Figure S3). Helical tilt angles in a related range have also been observed for dimers formed by the TMD of glycophorin or the amyloid precursor protein.[22,59,60] Unfortunately, it is difficult to further reduce the polypeptide content of the NMR samples because the NMR spectra shown typically required a day or more to acquire. Third, the possibility that the lipid properties may change upon addition of SM-C18, which by itself has a gel-to-liquid crystalline phase transition (45 °C)[46] above room temperature that was used in the experiments presented here and much higher than that of POPC (−2 °C), must be considered.[61] At low SM concentrations, the POPC/SM mixtures have been shown to remain in a liquid crystalline phase at ambient temperature.[48] When spectra have been recorded at low temperatures, considerably broadened liquid crystalline−gel phase transitions have to be considered where the phase transition temperature often represents a weighted average.[48,49] The phase behavior of the complex Golgi lipid mixture investigated here has to the best of our knowledge not yet been investigated. The modest changes in the side chain heterogeneity of A15 and A20 as well as the decrease in the side chain (and backbone) dynamics of V19, A20, and L23 could reflect a small decrease in membrane fluidity upon addition of SM-C18, point to direct molecular interactions, or both.

Therefore, it is of interest to also take into consideration the changes in the lipid properties that have been investigated by measuring the ^{31}P and ^{2}H solid-state NMR spectra of the phospholipids. The lipid order parameter provides information about the alignment and dynamics of the deuterated segments and has been used previously to study polypeptide−lipid interactions.[62,63] After deconvolution of the ^{2}H solid-state NMR spectra, the order parameter for each segment is obtained with the highest order parameters being associated with the CD_2 groups close to the glycerol backbone of the phospholipid.[64] The order parameter of the palmitoyl fatty acyl chain of POPC is hardly affected by the presence of either 1% p24TMD or 5% SM (Figure 8) in accordance with an only slight increase in the POPC-d_{31} order parameter in the presence of 50 mol % SM-C16.[65,66] However, when the peptide is added to a POPC/SM bilayer, a noticeable decrease in order parameter is observed, similar to the behavior of polypeptides that insert into the membrane interface.[62,63,67] Similar observations have been made with TM sequences of the MHC class II receptor.[68] These observations are suggestive that the somewhat tilted p24TMD shingomyelin interacts with SM-C18 in such a manner to exert positive curvature strain in the POPC membrane.

CONCLUSIONS

In the work presented here, the transmembrane domain of p24 was investigated by CD, fluorescence, and solid-state NMR spectroscopies. The degree of membrane insertion is heavily dependent on the exact phospholipid composition where in agreement with prior investigations[8] both the sphingomyelin headgroup and a fatty acyl chain length of 18 C atoms were found to be important (Figure 1E,F). In POPC or in mixed POPC/SM-C18 bilayers, the polypeptide adopts a helical structure (Figure 1E) that is oriented at a tilt angle of ∼19° (Figure 6). Whereas the oriented ^{15}N chemical shift and ^{2}H solid-state NMR spectra of most residues remain unaffected, small alterations are observed for the L23 and V18 sites (Figures 2−5 and 7), suggesting that only minor changes in conformation, topology, and dynamics occur due to the presence of 5 or 10 mol % SM-C18. It is likely that under conditions of this investigation (peptide-to-lipid ratio of 1% in POPC) the peptide occurs predominantly as a dimer. When the deuterium order parameters of POPC-d_{31} were investigated, the presence of SM-C18 or the polypeptide alone had little influence, but a considerable disordering effect was observed when they were added in combination.

ASSOCIATED CONTENT

Supporting Information

The Supporting Information is available free of charge on the ACS Publications website at DOI: 10.1021/acs.biochem.9b00375.

DOI: 10.1021/acs.biochem.9b00375
Biochemistry XXXX, XXX, XXX−XXX

Analytical data after peptide preparation and SDS−PAGE data of p24 in POPC membranes (PDF)

Accession Codes

p24 protein, UniProt entry Q15363 TMED2_HUMAN, residues 165−193.

AUTHOR INFORMATION

Corresponding Author

*Faculté de chimie, Institut le Bel, 4, rue Blaise Pascal, 67070 Strasbourg, France. Telephone: +33 3 68 85 13 03. E-mail: bechinge@unistra.fr.

ORCID

Burkhard Bechinger: 0000-0001-5719-6073

Author Contributions

†C.A. and P.K.-K. contributed equally to this work.

Funding

The financial contributions of the Agence Nationale de la Recherche (Projects ProLipIn 10-BLAN-731, membraneDNP 12-BSV5-0012, MemPepSyn 14-CE34-0001-01, InMembrane 15-CE11-0017-01, and the LabEx Chemistry of Complex Systems 10-LABX-0026_CSC), the University of Strasbourg, the CNRS, the Région Grand-Est (Alsace), and the RTRA International Center of Frontier Research in Chemistry are gratefully acknowledged.

Notes

The authors declare no competing financial interest.

ACKNOWLEDGMENTS

The authors are grateful to Britta Brügger, Felix Wieland, and their teams for most valuable discussions and for making data available prior to publication. Delphine Hatey helped with peptide synthesis. B.B. is grateful to the Institut Universitaire de France for providing additional time to be dedicated to research.

ABBREVIATIONS

CD, circular dichroism; CMC, critical micelle concentration; COPI, coat protein I; DMPC, 1,2-myristoyl-*sn*-glycero-3-phosphocholine; DPC, dodecylphosphocholine; FID, free induction decay; Fmoc, fluorenylmethoxycarbonyl; FRET, Förster resonance energy transfer; GPCR, G-protein-coupled receptor; HFIP, hexafluoroisopropanol; HPLC, high-performance liquid chromatography; LWHH, line width at half-height; MALDI, matrix-assisted laser desorption ionization; MD, molecular dynamics; NMR, nuclear magnetic resonance; P/L, peptide-to-lipid; PC, phosphatidylcholine; POPC, 1-palmitoyl-2-oleoyl-*sn*-glycero-3-phosphocholine; POPC, 1-palmitoyl-2-oleoyl-*sn*-glycero-3-phosphoethanolamine; POPS, 1-palmitoyl-2-oleoyl-*sn*-glycero-3-phospho-L-serine; SDS, sodium dodecyl sulfate; PAGE, polyacrylamide gel electrophoresis; SM, sphingomyelin; SM-C18, *N*-octadecanoyl-D-erythro-sphingosylphosphorylcholine; TFA, trifluoroacetic acid; TMD, transmembrane domain.

REFERENCES

(1) Strating, J. R., and Martens, G. J. (2009) The p24 family and selective transport processes at the ER-Golgi interface. *Biol. Cell 101*, 495−509.

(2) Popoff, V., Adolf, F., Brugger, B., and Wieland, F. (2011) COPI budding within the Golgi stack. *Cold Spring Harbor Perspect. Biol. 3*, No. a005231.

(3) Brugger, B., Sandhoff, R., Wegehingel, S., Gorgas, K., Malsam, J., Helms, J. B., Lehmann, W. D., Nickel, W., and Wieland, F. T. (2000) Evidence for segregation of sphingomyelin and cholesterol during formation of COPI-coated vesicles. *J. Cell Biol. 151*, 507−518.

(4) Dodonova, S. O., Diestelkoetter-Bachert, P., von Appen, A., Hagen, W. J., Beck, R., Beck, M., Wieland, F., and Briggs, J. A. (2015) VESICULAR TRANSPORT. A structure of the COPI coat and the role of coat proteins in membrane vesicle assembly. *Science 349*, 195−198.

(5) Pastor-Cantizano, N., Montesinos, J. C., Bernat-Silvestre, C., Marcote, M. J., and Aniento, F. (2016) p24 family proteins: key players in the regulation of trafficking along the secretory pathway. *Protoplasma 253*, 967−985.

(6) Denzel, A., Otto, F., Girod, A., Pepperkok, R., Watson, R., Rosewell, I., Bergeron, J. J., Solarie, R. C., and Owen, M. J. (2000) The p24 family member p23 is required for early embryonic development. *Curr. Biol. 10*, 55−58.

(7) Haberkant, P., Schmitt, O., Contreras, F. X., Thiele, C., Hanada, K., Sprong, H., Reinhard, C., Wieland, F. T., and Brugger, B. (2008) Protein-sphingolipid interactions within cellular membranes. *J. Lipid Res. 49*, 251−262.

(8) Contreras, F. X., Ernst, A. M., Haberkant, P., Björkholm, P., Lindahl, E., Gönen, B., Tischer, C., Elofsson, A., von Heijne, G., Thiele, C., Pepperkok, R., Wieland, F., and Brügger, B. (2012) Molecular recognition of a single sphingolipid species by a protein's transmembrane domain. *Nature 481*, 525−529.

(9) Ernst, A. M., Contreras, F. X., Thiele, C., Wieland, F., and Brugger, B. (2012) Mutual recognition of sphingolipid molecular species in membranes. *Biochim. Biophys. Acta, Biomembr. 1818*, 2616−2622.

(10) Ernst, A. M., and Brugger, B. (2014) Sphingolipids as modulators of membrane proteins. *Biochim. Biophys. Acta, Mol. Cell Biol. Lipids 1841*, 665−670.

(11) Bjorkholm, P., Ernst, A. M., Hacke, M., Wieland, F., Brugger, B., and von Heijne, G. (2014) Identification of novel sphingolipid-binding motifs in mammalian membrane proteins. *Biochim. Biophys. Acta, Biomembr. 1838*, 2066−2070.

(12) Bechinger, B., Resende, J. M., and Aisenbrey, C. (2011) The structural and topological analysis of membrane-associated polypeptides by oriented solid-state NMR spectroscopy: Established concepts and novel developments. *Biophys. Chem. 153*, 115−125.

(13) Naito, A., Matsumori, N., and Ramamoorthy, A. (2018) Dynamic membrane interactions of antibacterial and antifungal biomolecules, and amyloid peptides, revealed by solid-state NMR spectroscopy. *Biochim. Biophys. Acta, Gen. Subj. 1862*, 307−323.

(14) Gopinath, T., Mote, K. R., and Veglia, G. (2015) Simultaneous acquisition of 2D and 3D solid-state NMR experiments for sequential assignment of oriented membrane protein samples. *J. Biomol. NMR 62*, 53−61.

(15) Cross, T. A., Ekanayake, V., Paulino, J., and Wright, A. (2014) Solid state NMR: The essential technology for helical membrane protein structural characterization. *J. Magn. Reson. 239*, 100−109.

(16) Van Der Wel, P. C., Strandberg, E., Killian, J. A., and Koeppe, R. E. (2002) Geometry and intrinsic tilt of a tryptophan-anchored transmembrane alpha-helix determined by (2)H NMR. *Biophys. J. 83*, 1479−1488.

(17) Ramamoorthy, A., Wei, Y., and Lee, D. (2004) PISEMA Solid-State NMR Spectroscopy. *Annu. Rep. NMR Spectrosc. 52*, 1−52.

(18) Salnikov, E. S., Aisenbrey, C., Aussenac, F., Ouari, O., Sarrouj, H., Reiter, C., Tordo, P., Engelke, F., and Bechinger, B. (2016) Membrane topologies of the PGLa antimicrobial peptide and a transmembrane anchor sequence by Dynamic Nuclear Polarization/solid-state NMR spectroscopy. *Sci. Rep. 6*, 20895.

(19) Aisenbrey, C., and Bechinger, B. (2004) Tilt and rotational pitch angles of membrane-inserted polypeptides from combined 15N and 2H solid-state NMR spectroscopy. *Biochemistry 43*, 10502−10512.

(20) Michalek, M., Salnikov, E., and Bechinger, B. (2013) Structure and topology of the huntingtin 1−17 membrane anchor by a combined solution and solid-state NMR approach. *Biophys. J. 105*, 699−710.

(21) Resende, J. M., Verly, R. M., Aisenbrey, C., Cesar, A., Bertani, P., Pilo-Veloso, D., and Bechinger, B. (2014) Membrane interactions of Phylloseptin-1, −2, and −3 peptides by oriented solid-state NMR spectroscopy. *Biophys. J. 107*, 901−911.

DOI: 10.1021/acs.biochem.9b00375
Biochemistry XXXX, XXX, XXX−XXX

(22) Itkin, A., Salnikov, E. S., Aisenbrey, C., Raya, J., Glattard, E., Raussens, V., Ruysschaert, J. M., and Bechinger, B. (2017) Evidence for heterogeneous conformations of the gamma cleavage site within the amyloid precursor proteins transmembrane domain. *ACS Omega 2*, 6525−6534.
(23) Chu, S., Coey, A. T., and Lorigan, G. A. (2010) Solid-state (2)H and (15)N NMR studies of side-chain and backbone dynamics of phospholamban in lipid bilayers: investigation of the N27A mutation. *Biochim. Biophys. Acta, Biomembr. 1798*, 210−215.
(24) Aisenbrey, C., and Bechinger, B. (2004) Investigations of peptide rotational diffusion in aligned membranes by 2H and 15N solid-state NMR spectroscopy. *J. Am. Chem. Soc. 126*, 16676−16683.
(25) Bechinger, B., and Salnikov, E. S. (2012) The membrane interactions of antimicrobial peptides revealed by solid-state NMR spectroscopy. *Chem. Phys. Lipids 165*, 282−301.
(26) Henzler-Wildman, K. A., Martinez, G. V., Brown, M. F., and Ramamoorthy, A. (2004) Perturbation of the hydrophobic core of lipid bilayers by the human antimicrobial peptide LL-37. *Biochemistry 43*, 8459−8469.
(27) Kim, C., Spano, J., Park, E. K., and Wi, S. (2009) Evidence of pores and thinned lipid bilayers induced in oriented lipid membranes interacting with the antimicrobial peptides, magainin-2 and aurein-3.3. *Biochim. Biophys. Acta, Biomembr. 1788*, 1482−1496.
(28) Kemayo Koumkoua, P., Aisenbrey, C., Salnikov, E. S., Rifi, O., and Bechinger, B. (2014) On the design of supramolecular assemblies made of peptides and lipid bilayers. *J. Pept. Sci. 20*, 526−536.
(29) Kemayo-Koumkoua, P. (2015) Structural characterization of highly specific membrane protein-lipid interactions involved in cellular function. Ph.D. Thesis, University of Strasbourg, Strasbourg, France.
(30) Sreerama, N., and Woody, R. W. (2000) Estimation of protein secondary structure from circular dichroism spectra: comparison of CONTIN, SELCON, and CDSSTR methods with an expanded reference set. *Anal. Biochem. 287*, 252−260.
(31) Bechinger, B., and Opella, S. J. (1991) Flat-Coil Probe for NMR Spectroscopy of Oriented Membrane Samples. *J. Magn. Reson. 95*, 585−588.
(32) Bertani, P., Raya, J., and Bechinger, B. (2014) 15N chemical shift referencing in solid state NMR. *Solid State Nucl. Magn. Reson. 61−62*, 15−18.
(33) Rance, M., and Byrd, R. A. (1983) Obtaining High-Fidelity Spin-1/2 Powder Spectra in Anisotropic Media: Phase-Cycled Hahn Echo Spectroscopy. *J. Magn. Reson. 52*, 221−240.
(34) Davis, J. H., Jeffrey, K. R., Bloom, M., Valic, M. I., and Higgs, T. P. (1976) Quadrupolar Echo Deuteron Magnetic Resonance Spectroscopy in Ordered Hydrocarbon Chains. *Chem. Phys. Lett. 42*, 390−394.
(35) Koradi, R., Billeter, M., and Wüthrich, K. (1996) MOLMOL: a program for display and analysis of macromolecular structures. *J. Mol. Graphics 14*, 51−55.
(36) Salnikov, E., Bertani, P., Raap, J., and Bechinger, B. (2009) Analysis of the amide ^{15}N chemical shift tensor of the C(alpha) tetrasubstituted constituent of membrane-active peptaibols, the alpha-aminoisobutyric acid residue, compared to those of di- and tri-substituted proteinogenic amino acid residues. *J. Biomol. NMR 45*, 373−387.
(37) Aisenbrey, C., Sizun, C., Koch, J., Herget, M., Abele, U., Bechinger, B., and Tampe, R. (2006) Structure and dynamics of membrane-associated ICP47, a viral inhibitor of the MHC I antigen-processing machinery. *J. Biol. Chem. 281*, 30365−30372.
(38) Batchelder, L. S., Niu, H., and Torchia, D. A. (1983) Methyl reorientation in polycrystalline amino acids and peptides: A 2H NMR spin lattice relaxation study. *J. Am. Chem. Soc. 105*, 2228−2231.
(39) Aisenbrey, C., Michalek, M., Salnikov, E. S., and Bechinger, B. (2013) Solid-state NMR approaches to study protein structure and protein-lipid interactions. In *Lipid-Protein Interactions: Methods and Protocols* (Kleinschmidt, J. H., Ed.) pp 357−387, Springer, New York.
(40) Chipot, C., Dehez, F., Schnell, J. R., Zitzmann, N., Pebay-Peyroula, E., Catoire, L. J., Miroux, B., Kunji, E. R. S., Veglia, G., Cross, T. A., and Schanda, P. (2018) Perturbations of Native Membrane Protein Structure in Alkyl Phosphocholine Detergents: A Critical Assessment of NMR and Biophysical Studies. *Chem. Rev. 118*, 3559−3607.
(41) Aisenbrey, C., Marquette, A., and Bechinger, B. (2019) The Mechanisms of Action of Cationic Antimicrobial Peptides Refined by Novel Concepts from Biophysical Investigations. In *Antimicrobial Peptides, Advances in Experimental Medicine and Biology* (Matsuzaki, K., Ed.) Springer Nature, Singapore.
(42) Kollmitzer, B., Heftberger, P., Rappolt, M., and Pabst, G. (2013) Monolayer spontaneous curvature of raft-forming membrane lipids. *Soft Matter 9*, 10877−10884.
(43) Khemtemourian, L., Buchoux, S., Aussenac, F., and Dufourc, E. J. (2007) Dimerization of Neu/Erb2 transmembrane domain is controlled by membrane curvature. *Eur. Biophys. J. 36*, 107−112.
(44) Bechinger, B., and Sizun, C. (2003) Alignment and structural analysis of membrane polypeptides by 15N and 31P solid-state NMR spectroscopy. *Concepts Magn. Reson. 18A*, 130−145.
(45) Resende, J. M., Moraes, C. M., Munhoz, V. H. D. O., Aisenbrey, C., Verly, R. M., Bertani, P., Cesar, A., Pilo-Veloso, D., and Bechinger, B. (2009) Membrane structure and conformational changes of the antibiotic heterodimeric peptide distinctin by solid-state NMR spectroscopy. *Proc. Natl. Acad. Sci. U. S. A. 106*, 16639−16644.
(46) Maulik, P. R., and Shipley, G. G. (1996) Interactions of N-stearoyl sphingomyelin with cholesterol and dipalmitoylphosphatidylcholine in bilayer membranes. *Biophys. J. 70*, 2256−2265.
(47) Silvius, J. R. (1982) *Thermotropic Phase Transitions of Pure Lipids in Model Membranes and Their Modifications by Membrane Proteins*, John Wiley & Sons, New York.
(48) de Almeida, R. F., Fedorov, A., and Prieto, M. (2003) Sphingomyelin/phosphatidylcholine/cholesterol phase diagram: boundaries and composition of lipid rafts. *Biophys. J. 85*, 2406−2416.
(49) Pozo Navas, B., Lohner, K., Deutsch, G., Sevcsik, S., Riske, K. A., Dimova, R., Garidel, P., and Pabst, G. (2005) Composition dependence of vesicle morphology and mixing properties in a bacterial model membrane system. *Biochim. Biophys. Acta, Biomembr. 1716*, 40−48.
(50) Salnikov, E., Rosay, M., Pawsey, S., Ouari, O., Tordo, P., and Bechinger, B. (2010) Solid-state NMR spectroscopy of oriented membrane polypeptides at 100 K with signal enhancement by dynamic nuclear polarization. *J. Am. Chem. Soc. 132*, 5940−5941.
(51) Tiburu, E. K., Karp, E. S., Dave, P. C., Damodaran, K., and Lorigan, G. A. (2004) Investigating the dynamic properties of the transmembrane segment of phospholamban incorporated into phospholipid bilayers utilizing 2H and 15N solid-state NMR spectroscopy. *Biochemistry 43*, 13899−13909.
(52) Ferreira, H. E., and Drobny, G. P. (2017) Solid state deuterium NMR study of LKalpha14 peptide aggregation in biosilica. *Biointerphases 12*, 02D418.
(53) van Meer, G., Voelker, D. R., and Feigenson, G. W. (2008) Membrane lipids: where they are and how they behave. *Nat. Rev. Mol. Cell Biol. 9*, 112−124.
(54) Salnikov, E. S., Anantharamaiah, G. M., and Bechinger, B. (2018) Supramolecular Organization of Apolipoprotein-A-I-Derived Peptides within Disc-like Arrangements. *Biophys. J. 115*, 467−477.
(55) Partridge, A. W., Therien, A. G., and Deber, C. M. (2002) Polar mutations in membrane proteins as a biophysical basis for disease. *Biopolymers 66*, 350−358.
(56) Kinsey, R. A., Kintanar, A., Tsai, M. D., Smith, R. L., Janes, N., and Oldfield, E. (1981) First observation of amino acid side chain dynamics in membrane proteins using high field deuterium nuclear magnetic resonance spectroscopy. *J. Biol. Chem. 256*, 4146−4149.
(57) Keniry, M. A., Kintanar, A., Smith, R. L., Gutowsky, H. S., and Oldfield, E. (1984) Nuclear magnetic resonance studies of amino acids and proteins. Deuterium nuclear magnetic resonance relaxation of deuteriomethyl-labeled amino acids in crystals and in Halobacterium halobium and Escherichia coli cell membranes. *Biochemistry 23*, 288−298.
(58) Jenne, N., Frey, K., Brugger, B., and Wieland, F. T. (2002) Oligomeric state and stoichiometry of p24 proteins in the early secretory pathway. *J. Biol. Chem. 277*, 46504−46511.

DOI: 10.1021/acs.biochem.9b00375
Biochemistry XXXX, XXX, XXX−XXX

1142 (59) Sato, T., Tang, T. C., Reubins, G., Fei, J. Z., Fujimoto, T.,
1143 Kienlen-Campard, P., Constantinescu, S. N., Octave, J. N., Aimoto, S.,
1144 and Smith, S. O. (2009) A helix-to-coil transition at the epsilon-cut site
1145 in the transmembrane dimer of the amyloid precursor protein is
1146 required for proteolysis. *Proc. Natl. Acad. Sci. U. S. A. 106*, 1421−1426.
1147 (60) Smith, S. O., Eilers, M., Song, D., Crocker, E., Ying, W.,
1148 Groesbeek, M., Metz, G., Ziliox, M., and Aimoto, S. (2002)
1149 Implications of threonine hydrogen bonding in the glycophorin A
1150 transmembrane helix dimer. *Biophys. J. 82*, 2476−2486.
1151 (61) Harzer, U., and Bechinger, B. (2000) The alignment of lysine-
1152 anchored membrane peptides under conditions of hydrophobic
1153 mismatch: A CD, 15 N and 31 P solid-state NMR spectroscopy
1154 investigation. *Biochemistry 39*, 13106−13114.
1155 (62) Thennarasu, S., Tan, A., Penumatchu, R., Shelburne, C. E., Heyl,
1156 D. L., and Ramamoorthy, A. (2010) Antimicrobial and membrane
1157 disrupting activities of a peptide derived from the human cathelicidin
1158 antimicrobial peptide LL37. *Biophys. J. 98*, 248−257.
1159 (63) Salnikov, E. S., Mason, A. J., and Bechinger, B. (2009) Membrane
1160 order perturbation in the presence of antimicrobial peptides by 2H
1161 solid-state NMR spectroscopy. *Biochimie 91*, 734−743.
1162 (64) Seelig, J. (1977) Deuterium magnetic resonance: theory and
1163 application to lipid membranes. *Q. Rev. Biophys. 10*, 353−418.
1164 (65) Bunge, A., Muller, P., Stockl, M., Herrmann, A., and Huster, D.
1165 (2008) Characterization of the ternary mixture of sphingomyelin,
1166 POPC, and cholesterol: support for an inhomogeneous lipid
1167 distribution at high temperatures. *Biophys. J. 94*, 2680−2690.
1168 (66) Bartels, T., Lankalapalli, R. S., Bittman, R., Beyer, K., and Brown,
1169 M. F. (2008) Raftlike mixtures of sphingomyelin and cholesterol
1170 investigated by solid-state 2H NMR spectroscopy. *J. Am. Chem. Soc.*
1171 *130*, 14521−14532.
1172 (67) Michalek, M., Salnikov, E. S., Werten, S., and Bechinger, B.
1173 (2013) Membrane interactions of the amphipathic amino-terminus of
1174 huntingtin. *Biochemistry 52*, 847−858.
1175 (68) Aisenbrey, C., Salnikov, E., and Bechinger, B. (2019) Solid-state
1176 NMR investigations of the MHC II transmembrane domains −
1177 topological equilibria and lipid interactions. Submitted for publication.

DOI: 10.1021/acs.biochem.9b00375
Biochemistry XXXX, XXX, XXX−XXX